INTERNATIONAL JOURNAL OF INNOVATIVE RESEARCH & DEVELOPMENT

ISSN: 2278 – 0211 (Online)

Design And Performance Analysis Of Bump Surface In An Airfoil

Nithya S.
School Of Aeronautical Sciences, Hindustan University, India
G. Dineshkumar
School Of Aeronautical Sciences, Hindustan University, India

Abstract:
The performance of an airplane wing is often degraded by flow separation. Flow separation on an airfoil surface is related to the aerodynamic design of the airfoil profile. In order to obtain the best performance efficiencies for mission in aircraft, it is necessary to either: (a) alter the boundary layer behavior over the airfoil surface-flow control methods, or (b) change the geometry of the airfoil for changing free stream conditions- adaptive wing technology. The objective of this project work is to delay the flow separation point over the airfoil and increase the stall angle. This project deals about the effect of bump surface on the aircraft wing and also will give an over view of the results that is obtained for drag reduction by the creation of bump. In this paper the boundary layer and its controls are discussed.
After the airfoil profile generation and meshing the performance calculation had been carried out to evaluate the variation of angle of attacks, co-efficient of lift, and co-efficient of drag. The results obtained for with bump airfoil is compared with the airfoil without bump. The stall angle has increased from 23 to 24 by the creation of leading edge bump in an airfoil.
The designing of the airfoil with a bump and meshing is done by using GAMBIT. The analysis of fluid separation in an airfoil due to various locations of bumps and its effects on the aerodynamic forces is performed using FLUENT. This analysis is performed at a low velocity of 50m/s.

Key words: *Airfoil , Reynolds Number, Micro Air vehicles, Angle of attack, Flow separation, Stalling angle, Bump surface*

1.Nomenclature

ρ	=	density of air
ReC	=	chord Reynolds number
$m_{\text{int}ake}$	=	mass flow rate through intake
Re	=	Reynolds number
C_p	=	coefficient of pressure
α	=	Angle of attack
C_L	=	Coefficient of lift
C	=	chord length of airfoils
M_∞	=	Free stream Mach number
P	=	static pressure
μ	=	dynamic viscosity
P_0	=	STAGNATION PRESSURE

1.Introduction

When a real fluid flows past a solid boundary a layer of fluid which comes in contact with the boundary surface adheres to it on account of viscosity. Since this layer of fluid cannot slip away from the boundary surface it attains the same velocity as that of the boundary. In other wards at the boundary surface there is no relative motion between the fluid and the boundary. If the boundary is stationary, the fluid velocity at the boundary surface will be zero. Thus at the boundary surface the layer of fluid undergoes retardation. This retarded layer of fluid causes retardation for the adjacent layer of the fluid, thereby developing a small region in the

immediate vicinity of the boundary surface in which the velocity of flowing fluid increases gradually from zero at the boundary surface to the velocity of the mainstream. This region is known as boundary layer. The boundary layer develops, up to a certain portion of the plate from the leading edge, the flow in the boundary layer exhibits all the characteristics of laminar flow. This is so irrespective of whether the flow of the incoming stream is laminar or turbulent. This is known as laminar boundary layer. If the plate is sufficiently long, then beyond some distance from the leading edge the laminar boundary layer becomes unstable and then turbulent boundary layer is formed. This turbulent boundary layer may be formed by using external disturbance like passing outside a series of cylinder near the leading edge. The boundary layer thickness is considerable affected by the pressure gradient in the direction of flow. If the pressure gradient is zero, then the boundary layer continues to grow in thickness along a flat plate. With negative pressure gradient, the boundary layer tends to be reduced in thickness. With positive pressure gradient, the boundary layer thickens rapidly. The adverse pressure gradient plus the boundary shear decreases the momentum in the boundary layer, and if they both act over a sufficient distance they cause the fluid in the boundary layer to come to rest. In this position the flow separation is started. Also when the velocity gradient reaches to zero then the flow becomes to separate. So when the momentum of the layers near the surface is reduced to zero by the combined action of pressure and viscous forces then separation occur. So boundary layer separates under adverse pressure gradient as well as zero velocity gradient. Fluid flow separation can be controlled by various ways such as motion of the solid wall, slit suction, tangential blowing and suction, continuous suction and blowing by external disturbances, providing bumpy the surface/surface roughness etc. Among them here the surface roughness method is used to control flow the flow separation. The proposed method of flow control here is in introducing “large-scale” roughness to the upper surface of airfoil, such that the resultant shape would have a minor change in curvature. Due to this manufacturing constraint, the NACA 4412, a relatively thick airfoil, was selected.

2.Literature Review

2.1.Md. Abdul Ghani Mollah and Md. Farhad Hossain (1996) were designed and tested a new design of an actuator which can achieve a wide range velocity of without frequency dependence, is free of oscillating components as well as free of secondary frequencies**.** Sharp edge airfoils suffer from separation even at low angles of attack such as 8°, because the flow cannot negotiate the sharp turn at the leading edge. As the flow separates, the airfoil behaves as a bluff body. Due to this separation, a reduction in lift will be experienced by the airfoil due to the fact that the airflow on the suction side of the airfoil is separated and vortex shedding starts. The purpose of this research was to develop a flow control mechanism that could generate a pulsing jet along a slotted nozzle to increase the lift of circular-arc airfoils. A novel pulsing jet actuator was designed and constructed. The design proved that uniform and more powerful pulsing jets could be generated along the span of the airfoil. In addition, this actuator did not generate nonlinear interactions. The unsteady blowing right at the leading edge of a sharp-edged circular arc airfoil allows the management of the separated flow, leading to averaged pressure distributions that correspond to higher lift. This was shown to be due to convecting vortices, as detected in the form of a low pressure travelling wave. Significant improvement was obtained in the lift coefficient.

2.2.Md. Abdullah Al Bari, Mohammad Mashud and Hasan Ali (2012).
The aim of the research was to control the flow separation of an airfoil by providing a partial bumpy on the upper surface. In order to obtain the highest levels of performance efficiencies for mission varying aircraft, it is necessary to either: (a) alter the boundary layer behaviour over the airfoil surface-flow control methods of interest here, and/or (b) change the geometry of the air-foil real time for changing free stream conditions- of adaptive wing technology. Geometry the airfoil can be changed by providing bumpy on the upper surface. To investigate the effect of introducing large scale surface roughness through static curvature modifications on the low speed flow over an airfoil, two types model are prepared. One is regular surface model another is bumpy surface model. All the models are prepared by wood and the experiments are conducted using 36×36×100 cm subsonic wind tunnel. From the experimental investigations it has been observed that the flow separation on the airfoil can be delayed by using the bumpy on the upper surface. Flow separation occurs at 8° angle of attack in the smooth surface. But in bumpy surface it occurs at 14° angle of attack. That indicates the bumpy surface successfully controls the flow separation and increases the lift force of an airfoil.

2.3.Existing project

Wing fences, also known as boundary layer fences and potential fences are fixed aerodynamic devices attached to aircraft wings. Not to be confused with wingtip fences, wing fences are flat plates fixed to the upper surfaces (and often wrapping around the leading edge) parallel to the airflow. They are often seen on swept-wing aircraft. They obstruct span-wise airflow along the wing, and prevent the entire wing from stalling at once.
As a swept-wing aircraft slows toward the stall speed of the wing, the angle of the leading edge forces some of the airflow sidewise, toward the wing tip. This process is progressive, airflow near the middle of the wing is affected not only by the leading edge angle, but also the spanwise airflow from the wing root. At the wing tip the airflow can end up being almost all spanwise, as opposed to front-to-back over the wing, meaning that the effective airspeed drops well below the stall. Because the geometry of swept wings typically places the wingtips of an aircraft aft of its centre of gravity, lift generated at the wingtips tends to create a nose-down pitching moment. When the wingtips stall, both the lift and the associated nose-down pitching moment rapidly diminish. The loss of the nose-down pitching moment leaves the previously balanced aircraft with a net nose-up pitching moment. This forces the nose of

the aircraft up, increasing the angle of attack and leading to stall over a greater portion of the wing. The result is a rapid and powerful pitch-up followed by a complete stall, a difficult situation for a pilot to recover.

Figure 1: Fence Control

Wing fences delay, or eliminate, this effect by preventing the span wise flow from moving too far along the wing and gaining speed. When meeting the fence, the air is directed back over the wing surface. Similar solutions included a notch in the leading edge, as the use of slats, as on the later versions of the F-86. Slats can act as fences directly, in the form of their actuators, but also reduce the problem by improving the angle of attack response of the wing and moving the stall point to a lower speed.

3.Methodology

The computational steps in this project consist of three stages as shown in Figure 1. The project began from pre processing stage of geometry setup and grid generation. The geometry of the airfoil was obtained and the grid was generated by GAMBIT. The second stage was computational simulation by FLUENT solver using Finite Volume Approach. Finally is the post-processing stage where the aerodynamics characteristics of the bumps were found.

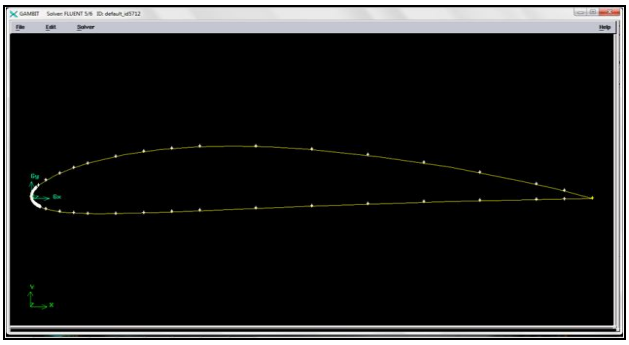

Figure 2: NACA 4412 Airfoil Co-Ordinates

The NACA 4412 airfoil profile was obtained by importing the airfoil coordinates to GAMBIT. The 2 dimensional structured quadrilateral mesh was utilized for computing the flow around the model because structured model is highly space efficient and Compared to structured meshes, the storage requirements for an unstructured mesh can be substantially larger since the neighborhood connectivity must be explicitly stored.

This meshing was done by using GAMBIT.

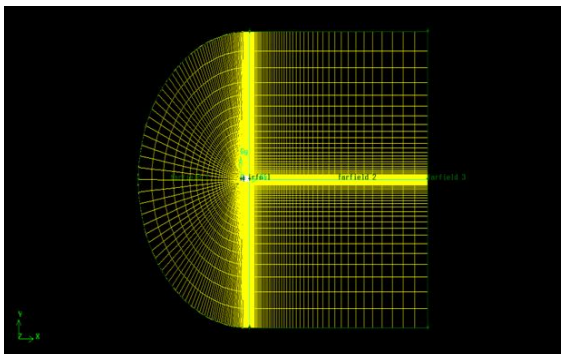

Figure 3: NACA 4412 Airfoil Meshed Geometry

The numerical simulation by the solver was made after the completion of the mesh generation. The solver formulation, turbulence model K – ω SST, boundary condition, solution control parameters and material properties were defined. After all the parameters were specified, the model was initialized. The initializing and iteration processes stopped after the completion of the computations. The results obtained were examined and analyzed.

4.Result And Discussion

Performance calculations have been carried out for various angle of attack. For each angle of attack Lift and Drag forces acting on airfoil is calculated by using these formulas

$L=\frac{1}{2}\rho v^2 s C_l$ ……..... (1)

$D=\frac{1}{2}\rho v^2 s\ C_{cl}$ …..... (2)

Density of air ρ = 1.22kg/m^3

Velocity of air = 50 m/s

Surface area = 1 m^2

Calculations

a) At angle of attack 23 without bump

C_l=1.3427 C_{cl} = 0.2980

$L=\frac{1}{2}\rho v^2 s\ C_l$ $D = \frac{1}{2}\rho v^2 s\ C_{cl}$

L=2047.6175N

D = 454.49575 N

L/D = 4.5052

b) At angle of attack 23 with bump at .1m

C_l=1.3775 C_{cl} = 0.29142

$L= \frac{1}{2}\rho v^2 s\ C_l$ $D = \frac{1}{2}\rho v^2 s\ C_{cl}$

L=2100.6875N

D = 444.4155N , L/D = 4.72

c) Angle of attack 23 with bump at .15 m

C_l=1.2865 C_{cl} = 0.28854

$L=\frac{1}{2}\rho v^2 s\ C_l$ $D = \frac{1}{2}\rho v^2 s\ C_{cl}$

L=1961.9125N

D = 440.0235N

L/D = 4.45865.

The result from the 2dimensional airfoil with bump model was compared to the 2-dimensional airfoil without bump. The discussions were focused on the aerodynamics characteristics which include drag coefficient CD, lift coefficient CL, and lift-to-drag ratio L/D. In addition, the pressure coefficient contours and path lines will also be observed and studied. The simulation was carried out at various angles of attack, α, and Mach number less than 0.2. NACA airfoil 4412 it stalled at 22 degree angle of attack. Thus, simulation was done between 18 and 24 degree angles of attack at 50 m/s velocity.

4.1.Lift Coefficient, Cl Analysis

Table 1 shows the lift coefficient C_l changes with angle of attack, α. for different bump locations and without bump model at velocity of 50 m/s..

S.NO	AOA	without bump	with bump at .1m	with bump at .15m
1	18	1.0652	1.0463	0.9258
2	20	1.2465	1.2376	1.1378
3	22	1.3713	1.3694	1.3071
4	23	1.3427	1.3775	1.2865
5	24	1.2943	1.3491	1.2039

Table 1: Lift Coefficient, C_l Comparison For Different Bump Locations

Figure1 shows the airfoil with bump at .1m has highest lift coefficient, C_l in comparison with other types of bump. The airfoil without bump gives the second highest lift coefficient, C_l. Both the airfoil without bump and with bump at .1m shows an increase in the lift coefficient, C_l. The airfoil with bump at .2m decreases the lift coefficient.

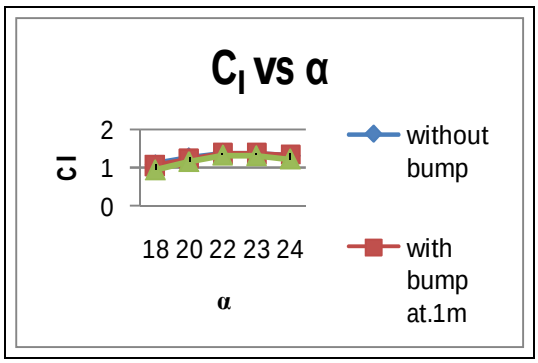

Fig. 4: Lift Coefficient, C_l Versus Angle Of Attack, A , And Velocity Of 50 M/S.

4.2.Drag Coefficient, Cd Analysis

Table 2 shows the drag coefficient C_d changes with angle of attack, α. for different bump locations and without bump model at velocity of 50 m/s. Table 2. Drag Coefficient, C_d Comparison for different bump locations.

S.NO	AOA	without bump	with bump at .1m	with bump at .15m
1	18	0.20927	0.22469	0.2256
2	20	0.24931	0.25784	0.2567
3	22	0.2682	0.27237	0.25375
4	23	0.29803	0.29142	0.28854
5	24	0.3127	0.31839	0.28854

Table 2: C_d vs angle of attack

Figure 2 shows the airfoil with bump at .15m has lowest drag coefficient, C_d in comparison with other types of bump. The airfoil without bump gives the second lowest drag coefficient, C_d. Both the airfoil without bump and with bump at .15m shows a decrease in the drag coefficient, C_d. The airfoil with bump at .2m increases the drag coefficient.

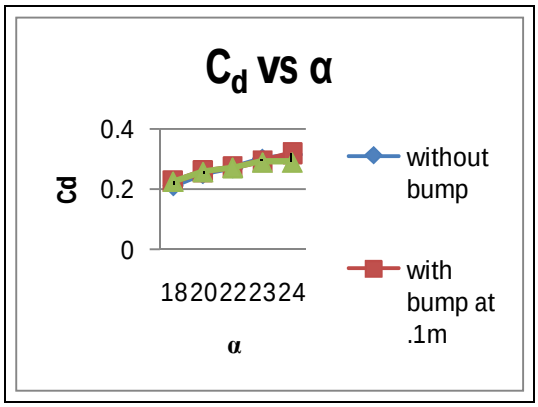

Figure 5: Drag Coefficient, C_d At Various Angle Attack, A And Velocity Of 50 M

4.3.Lift To Drag Ratio, C_l / C_d Analysis

Table 3 shows the lift to drag ratio C_l / C_d changes with angle of attack, α. for different bump locations and without bump model at velocity of 50m/s..

Figure 3 shows the airfoil with bump at .15m has highest lift to drag ratio C_l /C_d in comparison with other types of bump. The airfoil without bump gives the second highest lift to drag ratio, C_l / Cd. Both the airfoil without bump and with bump at .15m show an increase in the lift to drag ratio, C_l / C_d. The airfoil with bump at .2m decreases the lift to drag ratio.

S.NO	AOA	without bump	With bump at 0.1mc	with bump at .15mc
1	18	4.8579	4.6566	4.1
2	20	4.9997	4.7998	4.4324
3	22	5.11297	5.0277	4.9558
4	23	4.5052	4.7268	4.4586
5	24	4.13911	4.2372	3.9802

Table 3

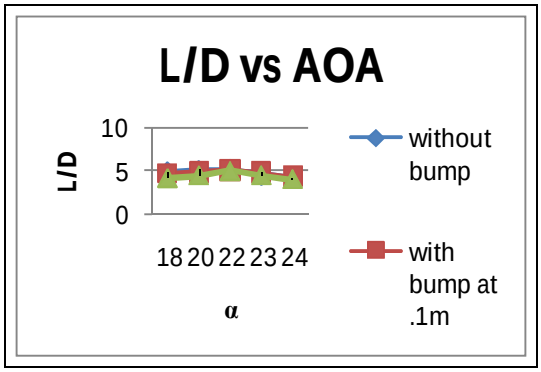

Figure 6: L/D At Various Angle Attacks, A And Velocity Of 50 M/S

4.4.Pressure, Velocity, Turbulence And Vector Contours

Figure 4 until 11 below show pressure, velocity, and turbulence and vector contours of airfoil with bump at maximum Table 3. Lift to drag ratio, C_l / C_d Comparison for different bump locations

velocity of 50 m /s and at 23 degree angle of attack. When the angle of attack, α increases, the upper surface will create a lower pressure coefficient. The high intensity blue area located on the upper surface suggests high lift is generated. At high angle of attack, α, lift is still capable of generating, but most of the total force is directed backward as drag.

Pressure contours

Fig. 7 Pressure Contours Respectively to without bump, bump at .1m and bump at.15m at α= 23

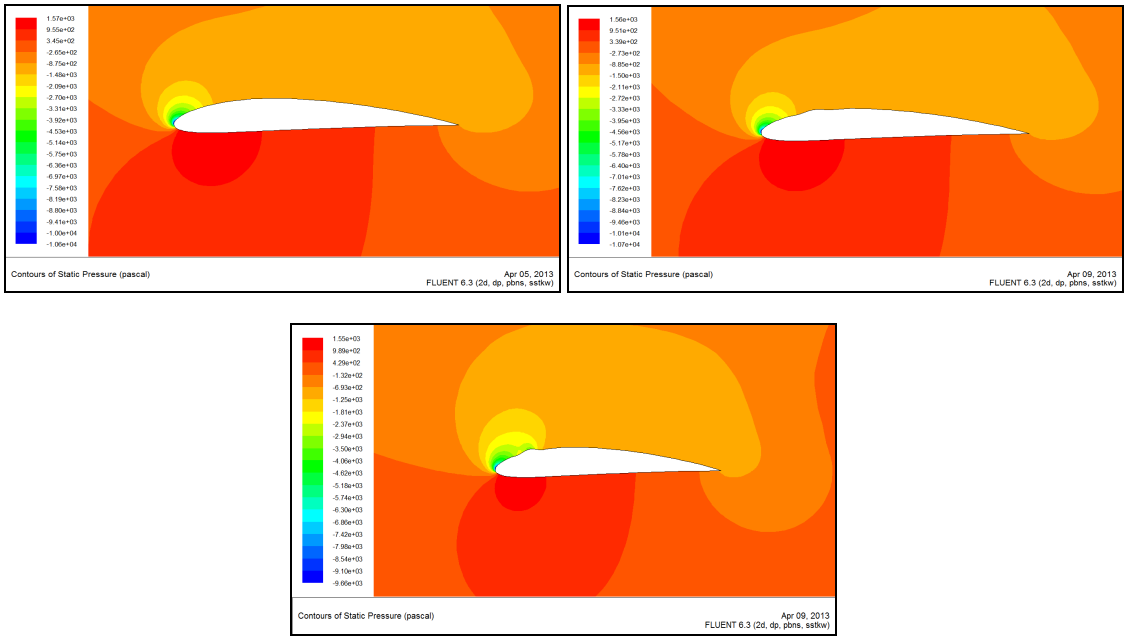

Velocity contours

Fig. 8 Velocity Contours respectively to without bump, bump at .1m and bump at .15m at α= 23

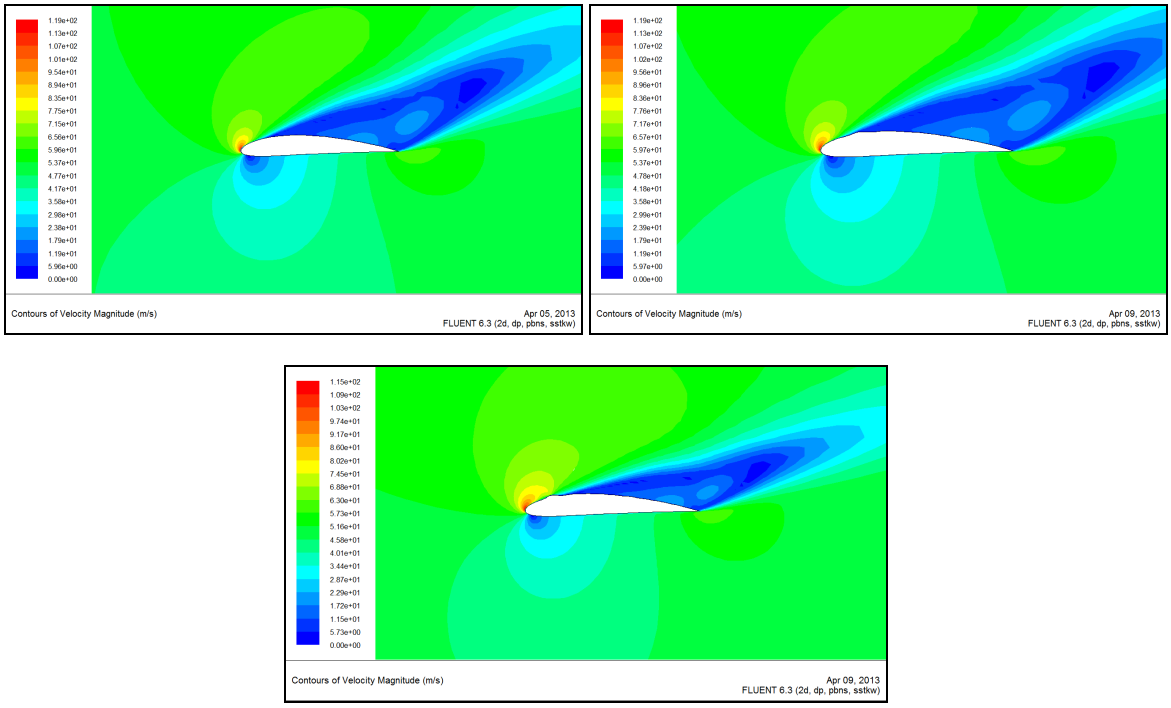

Static Pressure Plot

Fig. 9 Static Pressure Plots respectively to without bump, bump at .1m and bump at .15m at α= 23

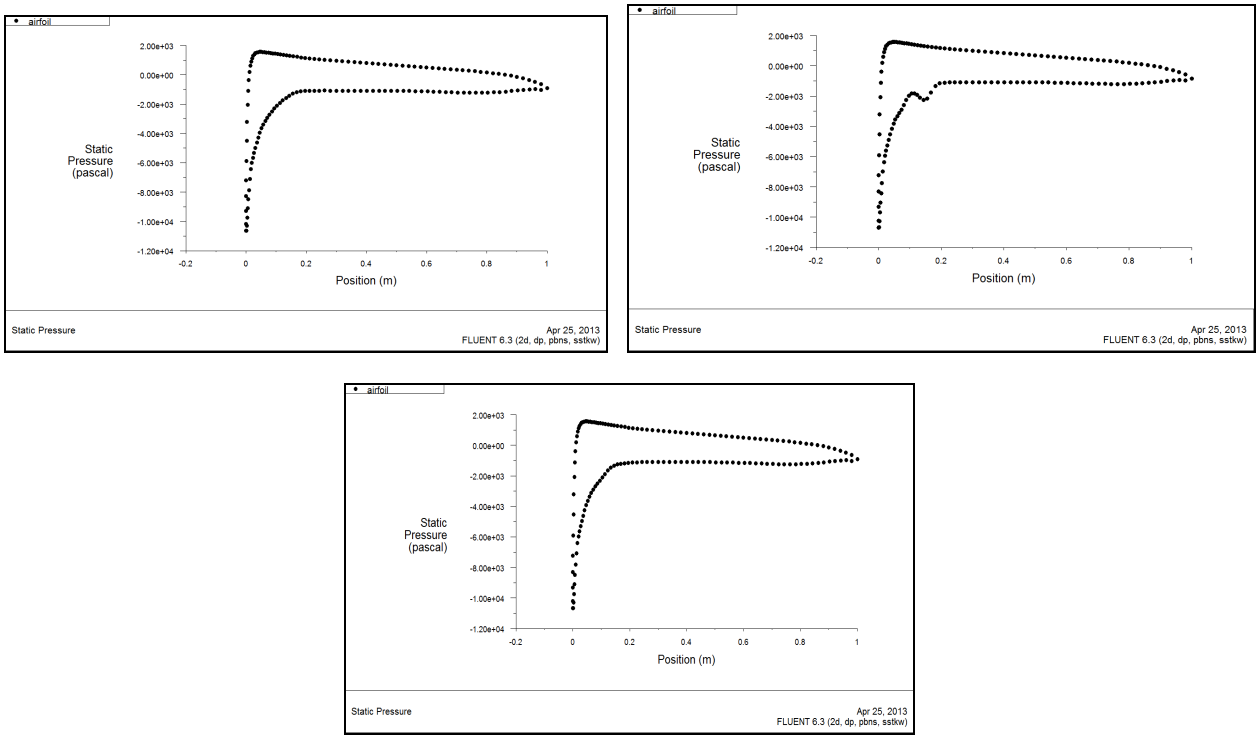

Turbulence contours

Fig. 10 Turbulence contours respectively to without bump, bump at .1m and bump at .15m at α= 23

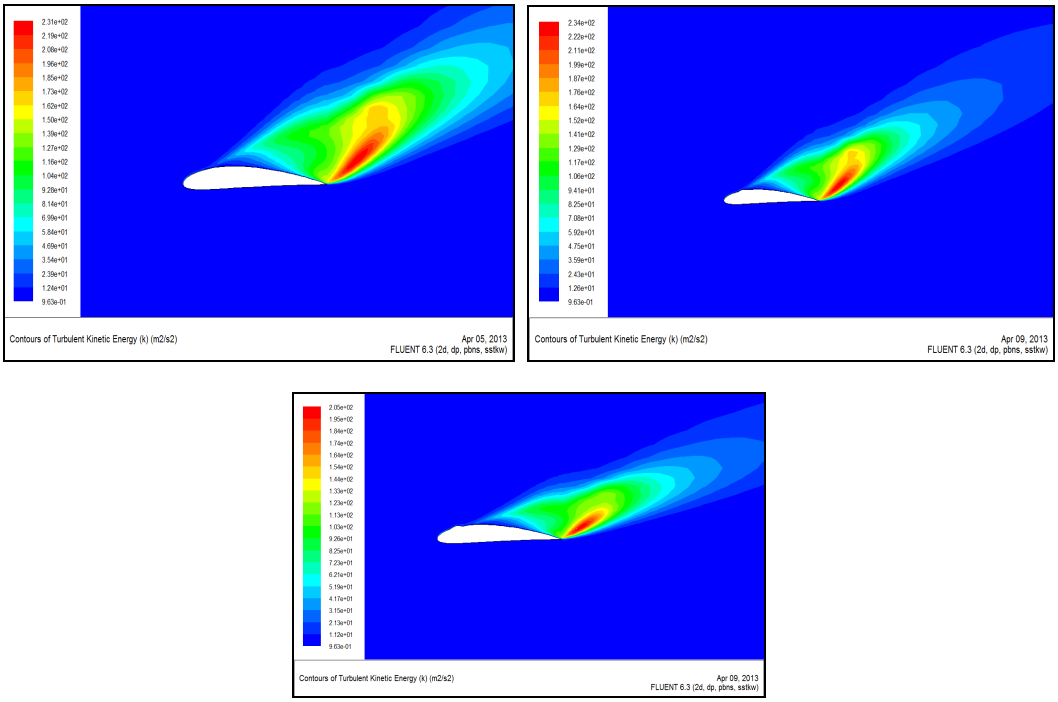

Vector Contours

Fig.11 Vector contours respectively to without bump, bump at .1m and bump at .15m at α= 23

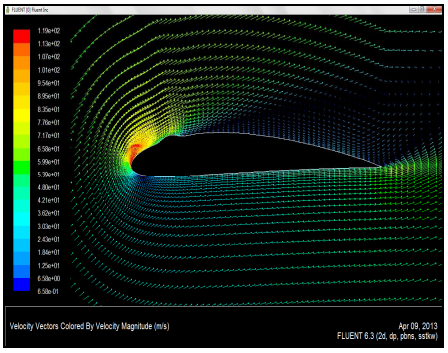

Path lines

From these comparisons of path lines for without bump and bump at two different locations clearly show the delayed boundary layer separation in the case of bump at .15m than without bump and others. Because of this separation point extension we can increase the lift of the wing and can obtain the better performance.

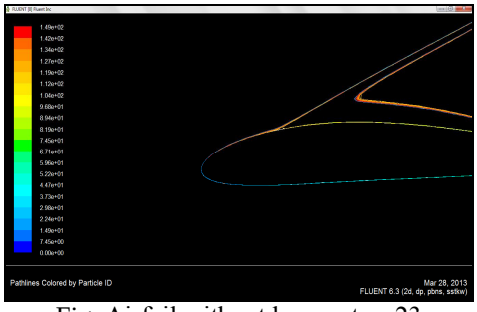

Fig. Airfoil without bump at α=23

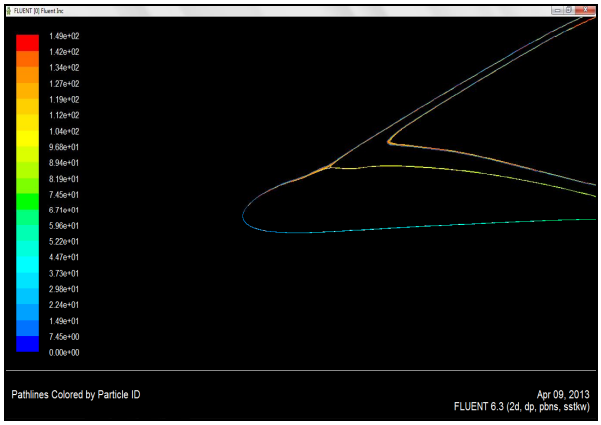

Fig Airfoil with bump at .15m and at α= 23

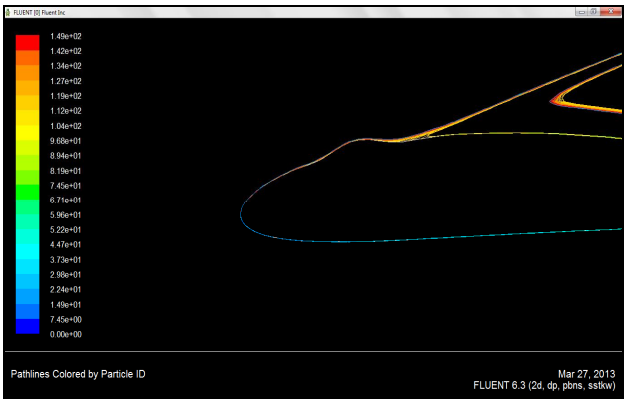

Fig Airfoil with bump at .1m and at α= 23

5.Future Enhancement And Conclusion

5.1.Future Recommendation

The lift coefficient is increased 3.4% by using this single bump concept at the location of .1m. the bump at 0.15m is not effective to reattach the flow because this bump is placed just away from the separation point. For obtaining the best result and know the effects and aerodynamic characteristic of bump we can analyse the model with multi bumps or fully bumpy model at various speed. Models are analyzed here and number of studies had been done at Low Reynolds number only. The experiment can be done at high Reynolds number to know the relationship between them because flow type depends Reynolds number. We can change the number of bumps, locations and dimensions of bump and can do the same experiment. If we use different flow solver then the accuracy of result can be checked to know the lift increment by the creation bumps on suction side of airfoil.

5.2.Advantages

- The size of this bump is comparatively small, but large enough to be manufactured
- Bump presence does not affect wing structure
- This gives outward movement only so it will not affect internal structure of the wing.
- Bump delays the stall angle by delaying the flow separation point
- During take-off at low air speed the only way to increase the lift is increase the angle of attack. Bump will be beneficial for this purpose.

5.3.Disadvantages

- Bump will be effective at high angle of attack only. At a low angle of attack which reduces the lift instead of increase the lift.
- Special care should be taken to the size and location of bumps to avoid affecting the control surfaces, and restrict them to outward movements only.
- They also modify the handling and stability characteristics

5.4.Limitation

- Bump size and location should be considered.
- Bump height must be in appropriate height. Should not be less than .2%c and greater than 2%c otherwise it will be ineffective.
- For better results we can use this bump concept at high angle of attack only
- Study carried out only at sea level conditions.

5.5.Conclusion

The basic about the boundary layer, their separation effects in aircraft performance and ways to reduce and delay the flow separation were studied and the suitable way to delay the boundary layer flow separation is selected for the project. The bump surface at certain location near to the leading edge will increase the stall point. In this project the bump location at .1m have given better performance than the without bump case and the bump at .15m. From that we can know that the location of bumps plays an important role the bump in an ineffective location will give negative results only.. The stall angle of NACA 4412 airfoil is 22 but 24 for the airfoil with bump at .1m and 3.4% lift increment is obtained because at stall angle or high angle of attack the bump can reattach the flow where the flow separation starts. So it will increase the lift and increase the stall angle.

6.References

1. Abu-Ghannam, B.J. and Shaw, R., "Natural transition of boundary layers-the effect of turbulence, pressure gradient and flow history" Journal of Mechanical Engineering Science, 1980, Vol. 22, No. 5, pp. 213-228.
2. Anderson,J.D.Jr.,"Fundamentals of Aerodynamics" Second Edition, New York: Mcgraw-Hill, Inc, 1991.
3. Battle, J.M., Hydrodynamic design of the humpback whale flipper, Journal of Morphology, Pennsylvania, pp.51-60, 1995.
4. Bingham, G.J. and Chen, A.W, "Low-speed aerodynamic characteristics of an aerofoil optimized for maximum lift coefficient" NASA TN D-7071, 1972.
5. Catalin Nae, "Synthetic Jets Influence on NACA 0012 Airfoil at High, Angles of Attack", AIAA Atmospheric Flight Mechanics Conference and Exhibit, Boston, Massachusetts, August 10-12, 1998.
6. Cebeci, T., Mosinskis, G.J. and Smith A.M.O, "Calculation of separation points in ıncompressible turbulent flows", Journal of Aircraft, 1972, Vol. 9, No. 9, pp. 618-624.
7. Custodio D. and Levshin, A., Effects of leading-edge protuberances on airfoil performance, AIAA Journal, 45(11), pp. 2634-2642, 2007
8. Dannenberg, R. E., and Weiberg, J. A., "Section Characteristics of a 10.5-Percent Thick Airfoil with Area Suction as Affected by Chordwise Distribution of Permeability," NASA TN 2847, Dec. 1952.
9. Drela, M. and Giles, M.B., "Viscous-inviscid analysis of transonic and low Reynolds number aerofoils" AIAA Journal, 1987, Vol. 25, No. 10, pp. 1347-1355.
10. Genç M.S., Lock G. and Kaynak U., An Experimental and Computational Study of Low Re Number Transitional Flows over an Aerofoil with Leading Edge Slat, AIAA-2008
11. Genç, M.S., Kaynak, Lock, G., Flow over an aerofoil without and with leading edge slat at a transitional Reynolds number, Pro.Ins Mech.Eng, Part G-Journal of Aerospace Engineering, in press.
12. Godard, G. and Stanislas, M., Control of a Decelerating Boundary Layer. Part 1: Optimization of Passive Vortex Generators, Aerospace Science and Technology, 10(3), pp. 181-191, 2006.
13. Hefner, J.N., Bushnell, D.M., Viscous Drag Reduction via Surface Mass Injection, in: Viscous Drag Reduction in Boundary Layers, Progress in Astronautics and Aeronautics, Volume 123, 1990
14. Huang L., Huang P. G. and LeBeau R. P., Numerical Study of Blowing and Suction Control Mechanism on NACA0012 Airfoil, Journal of Aircraft ,vol. 41, No. 1, January–February 2004.
15. Khorrami, M. R., Berkman, M. E. & Choudhari, M. 2000 Unsteady flow computations of a slat with blunt trailing edge. AIAA Journal 38 (11), 2050–2058.
16. Liebeck, R.H. and Ormsbee, A.I., "Optimization of aerofoils for maximum lift" Journal of Aircraft, 1970, Vol. 7, No. 9-10, pp. 409-415.
17. Liebeck, R.H., "A class of aerofoils designed for high lift in incompressible flow", Journal of Aircraft, 1973, Vol. 10, No. 10, pp. 610-617.
18. Langtry, R.B. and Menter, F.R. "Transition modeling for general CFD applications in aeronautics" AIAA Paper 2005-0522, 2005.
19. Mahmood, S. and Radespiel, R., RANS simulation of jet actuation in a boundary layer-flow using chimera grids, GermanAerospace Congress, 2009.